Journal of Engineering Mathematics **49:** 181–193, 2004.

The Helmholtz equation for convection in two-dimensional porous cavities with conducting boundaries

D. ANDREW REES and PEDER A. TYVAND[1]
Department of Mechanical Engineering, University of Bath, Claverton Down, Bath, BA2 7AY, UK (e-mail: ensdasr@bath.ac.uk); [1]*Department of Agricultural Engineering Agricultural University of Norway, 1432 Ås, Norway (e-mail: peder.tyvand@itf.nlh.no)*

Received 20 March 2003; accepted in revised form 6 November 2003

Abstract. It is well-known that every two-dimensional porous cavity with a conducting and impermeable boundary is degenerate, as it has two different eigensolutions at the onset of convection. In this paper it is demonstrated that the eigenvalue problem obtained from a linear stability analysis may be reduced to a second-order problem governed by the Helmholtz equation, after separating out a Fourier component. This separated Fourier component implies a constant wavelength of disturbance at the onset of convection, although the phase remains arbitrary. The Helmholtz equation governs the critical Rayleigh number, and makes it independent of the orientation of the porous cavity. Finite-difference solutions of the eigenvalue problem for the onset of convection are presented for various geometries. Comparisons are made with the known solutions for a rectangle and a circle, and analytical solutions of the Helmholtz equation are given for many different domains.

Key words: conducting boundaries, degeneracy, Helmholtz equation, onset of convection, porous media

1. Introduction

Thermal convection in a saturated porous medium heated from below was first investigated by Horton and Rogers [1]. They determined the critical Rayleigh number, $4\pi^2$, for a porous layer of infinite horizontal extent and showed that the associated convection cell is a two-dimensional roll with square cross-section. These results for the onset of convection were confirmed by Lapwood [2]. The above early papers assumed that the upper and lower surfaces are impermeable and perfectly conducting, but Nield [3] supplemented their linear stability analyses with two alternative boundary conditions: the conditions of constant heat flux and the condition of a permeable surface subject to constant pressure; see also Nield and Bejan [4, p. 181] who presented a table with all possible combination of permeable/impermeable conditions and conducting/constant flux conditions at the top and bottom.

The early papers also assumed that the layer is of infinite horizontal extent so that the horizontal eigenfunction is a pure Fourier mode. Beck [5] generalized the Horton-Rogers-Lapwood problem to a finite rectangular box, but he assumed thermally insulating and impermeable lateral walls. In these cases the pure Fourier modes persist as the horizontal eigenfunctions. The first paper which presented exact analytical solutions with more complicated horizontal eigenfunctions was written by Nilsen and Storesletten [6]. Their results were confirmed by Rees and Lage [7], who also extended that analysis into the weakly nonlinear regime. These papers gave the onset criterion for two-dimensional convection in a rectangular box with conducting sidewalls, where the temperature perturbation is zero.

Nilsen and Storesletten [6] found two remarkable qualitative differences from the problem considered by Beck [5]: (i) the critical Rayleigh number is a smooth monotonic function of the aspect ratio of the box and (ii) the eigenvalue problem is degenerate for all aspect ratios. This means that the most unstable mode of disturbance may be represented by two different stream functions and two different temperature perturbations at onset. The streamlines from the first mode correspond to the isotherms of the second mode, and vice versa. Lyubimov [8] and Bratsun *et al.* [9] showed that this degeneracy occurs for a two-dimensional porous medium with zero perturbation along a contour of arbitrary shape, although no solutions were given.

Storesletten and Tveitereid [10] also found that the same degeneracy is present in the two-dimensional onset problem for a horizontal circular cylinder. Their solution was only numerical in terms of truncated Taylor series.

We will show that the degeneracy of the eigenvalue problem for a porous cylinder with zero perturbation temperature along the boundary leads to a Helmholtz equation governing the onset of convection. We will perform finite-difference simulations to illustrate the degeneracy, and compare with analytical solutions of the Helmholtz equation.

2. Basic equations

We consider a two-dimensional porous cavity with a homogeneous and isotropic permeability K. Cartesian coordinates x, y are introduced, where the y-axis points vertically upwards. The temperature field is $T(x, y, t)$, where t denotes time. A steady temperature field $T_s(y)$ is prescribed along the boundary of the porous medium, and from the heat equation it follows that T_s must vary linearly in the vertical direction to achieve steady conditions, where the unperturbed temperature field is given by $T = T_s(y)$ everywhere inside the porous medium. This temperature distribution along the boundary is maintained even when the internal temperature field has been perturbed. This means that the perturbation temperature $\theta(x, y, t)$ is assumed to vanish along the entire boundary of the cavity, *i.e.*,

$$\theta = 0 \ \text{ along the boundary contour.} \tag{2.1}$$

This thermal boundary condition is, for simplicity, called a “conducting boundary", even though the conducting properties at such a boundary are clear only in some simple cases. Storesletten and Tveitereid [10] showed that this condition represents a highly conducting solid medium surrounding a circular porous cavity of much smaller conductivity. However, we note that horizontal isotherms arise in such a circular cylinder for all conductivity ratios. Nilsen and Storesletten [6] investigated the horizontal rectangle, where this condition represents a wall that is a much better conductor than the porous medium, but still considerably less conductive than the top and bottom planes.

We introduce a length scale H which is usually the largest diameter of the porous cavity. Since we are going to consider different orientations of a given porous cavity, we stress that H is a fixed length for a given configuration and therefore the definition of H does not vary with the orientation.

We choose the following units for dimensionless time, velocity and pressure:

$$(c_p\rho)_m H^2/k_m, \quad \kappa_m/H, \quad \rho_0 \nu \kappa_m/K, \tag{2.2}$$

respectively, where c_p is the specific heat at constant pressure, k is the heat conductivity, κ is the thermal diffusivity, ν is the kinematic viscosity of the saturating fluid, and ρ_0 is a reference fluid density. The subscript m represents the mixture of solid and fluid.

The dimensionless Darcy-Boussinesq equations for convection in a homogeneous and isotropic porous medium are given by:

$$\mathbf{v} + \nabla p - \mathrm{Ra} T \mathbf{j} = 0, \tag{2.3}$$

$$\nabla \cdot \mathbf{v} = 0, \tag{2.4}$$

$$\frac{\partial T}{\partial t} + \mathbf{v} \cdot \nabla T = \nabla^2 T. \tag{2.5}$$

The Rayleigh number for a porous medium is given by

$$\mathrm{Ra} = \frac{g\beta K \Delta T H}{\nu \alpha_m}. \tag{2.6}$$

Here we have introduced ΔT, which is defined as the temperature difference over a vertical distance H. This means that the temperature gradient in the basic unperturbed steady state must be considered to be fixed when a given cavity has been rotated with respect to the gravity field. Thus ΔT must not be interpreted as the temperature difference between the lowest and highest point on a boundary. We have also introduced g as the gravitational acceleration and β as the expansion coefficient. In Equations (2.3)–(2.5), $\mathbf{v}$ is the velocity, while p is the pressure, and $\mathbf{j}$ is the vertical unit vector. The basic dimensionless temperature gradient is -1 and is due to pure conduction. We perturb the basic temperature field and introduce the temperature perturbation $\theta(x, y, t)$ as follows:

$$T = -y + \theta(x, y, t). \tag{2.7}$$

We will assume that the onset of convection is given by a stationary mode, rather than as an oscillatory mode; the proof of exchange of stabilities is straightforward in the present context and is omitted.

We introduce the stream function ψ and eliminate the pressure. After linearisation the governing equations are

$$\nabla^2 \psi - \mathrm{Ra} \frac{\partial \theta}{\partial x} = 0, \qquad \text{and} \qquad \nabla^2 \theta + \frac{\partial \psi}{\partial x} = \frac{\partial \theta}{\partial t}, \tag{2.8}$$

where the velocity components are $(-\partial\psi/\partial y, \partial\psi/\partial x)$. It may be shown easily that exchange of stabilities applies and therefore the criterion for the onset of convection may be obtained by solving the partial differential eigenvalue problem which is found by setting to zero the time derivative in (2.8).

A modified complex stream function Ψ may be defined as

$$\psi = \mathrm{i}\sqrt{\mathrm{Ra}}\Psi \tag{2.9}$$

and the resulting coupled equations for θ and Ψ are

$$\nabla^2 \Psi + \mathrm{i}\sqrt{\mathrm{Ra}} \frac{\partial \theta}{\partial x} = 0, \qquad \text{and} \qquad \nabla^2 \theta + \mathrm{i}\sqrt{\mathrm{Ra}} \frac{\partial \Psi}{\partial x} = 0, \tag{2.10}$$

where the conditions

$$\Psi = \theta = 0 \ \text{ along the boundary} \tag{2.11}$$

correspond to impermeable and conducting boundaries. We conclude that the coupled eigenvalue problem is completely symmetric in Ψ and θ. If we eliminate θ to formulate the eigenvalue problem in terms of Ψ alone, then this will be identical to the problem written in terms of θ which we get by eliminating Ψ. Such eliminations lead to

$$\nabla^4\Psi + \mathrm{Ra}\frac{\partial^2\Psi}{\partial x^2} = 0 \qquad \text{and} \qquad \nabla^4\theta + \mathrm{Ra}\frac{\partial^2\theta}{\partial x^2} = 0. \tag{2.12}$$

This complete symmetry in Ψ and θ implies that the solutions must be the same, *i.e.*,

$$\Psi(x, y) = \theta(x, y), \tag{2.13}$$

provided that there is a unique solution of this complex eigenvalue problem given by (2.10) and (2.11).

Given that (2.10) and (2.11) form an eigenvalue problem, the solution is subject to an arbitrary complex amplitude, which we call A. Later we will see that the significance of the factor A is to determine the precise location of the cell walls (*i.e.*, the locations where the stream function is zero and which divide regions of flow circulating in opposite directions). Although the position of the cell walls will be arbitrary, since these will depend on the argument of A, their mutual separation will be constant for any given shape of cavity.

Given that the relationship between the original streamfunction and the temperature is

$$\psi(x, y) = i\sqrt{\mathrm{Ra}}\,\theta(x, y). \tag{2.14}$$

there is an inherent phase shift of $\pi/2$ between the streamlines and their associated isotherms. It manifests itself when we take the real and imaginary parts of the complex solution. If, for a given choice of A, an eigensolution is such that the real part is the temperature then the imaginary part is the associated stream function. If we now replace the complex amplitude A by $\mathrm{i}A$, the imaginary part will be the temperature and the negative of the real part will be the stream function.

We eliminate Ψ by (2.13), and reduce the eigenvalue problem (2.10)–(2.11) to a second-order problem:

$$\nabla^2\theta + \mathrm{i}\sqrt{\mathrm{Ra}}\frac{\partial\theta}{\partial x} = 0, \tag{2.15}$$

$$\theta = 0 \ \text{ along the boundary} \tag{2.16}$$

It is important that θ represents the physical temperature. This requires that θ must be governed by a real eigenvalue problem. The way to achieve this, is to separate out a Fourier component as follows:

$$\theta = F(x, y)\ \mathrm{e}^{-\mathrm{i}\alpha\pi x}, \tag{2.17}$$

where the function $F(x, y)$ is assumed to be real. Insertion of (2.17) into the governing equation (2.15) and the taking the real and imaginary parts leads to two equations:

$$\nabla^2 F - \alpha^2\pi^2 F + \sqrt{\mathrm{Ra}}\alpha\pi F = 0, \tag{2.18}$$

$$\sqrt{\mathrm{Ra}} = 2\alpha\pi. \tag{2.19}$$

The eigenvalue problem for $F(x, y)$ is now governed by the Helmholtz equation

$$\nabla^2 F + \alpha^2 \pi^2 F = 0, \tag{2.20}$$

with the boundary condition

$$F = 0 \text{ on the boundary.} \tag{2.21}$$

Now the solution $F(x, y)$ may be made complex, but only because we could use an arbitrary complex amplitude. The eigenvalue α is a dimensionless wavenumber which measures the number of cells per unit horizontal length. The eigenvalue problem given by (2.20)–(2.21) will have an infinite number of nontrivial solutions, but we will concentrate on that eigensolution which has the smallest value of α, termed $\alpha_{\min}$, and which produces the critical Rayleigh number

$$\mathrm{Ra}_c = 4\alpha_{\min}^2 \pi^2. \tag{2.22}$$

Since the Laplacian operator is independent of orientation, the Helmholtz eigenvalue problem is independent of the orientation of the porous cavity. This means that the critical Rayleigh number Ra and the associated wavenumber α are the same for all orientations of a given cavity shape in the vertical plane. The isotherm and streamline pattern, however, will change with orientation because ψ and θ always involve the factor $\mathrm{e}^{-\mathrm{i}\alpha\pi x}$. Cell walls are therefore always vertical, but the horizontal distance $1/\alpha$ between neighbouring cells will be independent of orientation. The complex form of the solution (2.17) ensures that the isotherm pattern has vertical walls displaced a horizontal distance $1/(2\alpha)$ away from the cell-walls of the streamline pattern. Moreover, the solution is degenerate in that the isotherm and streamline patterns may be interchanged. More generally, the location of cell walls may be regarded as being located arbitrarily since F may have an arbitrary complex phase.

3. Numerical method

The partial differential eigenvalue problem given by Equations (2.8) was solved by first applying standard second-order accurate central-difference approximations, and then applying the inverse-power method to obtain the eigenvalue, Ra, of smallest magnitude.

The power method and the inverse-power methods are well-known methods for obtaining the eigenvalue of largest and smallest magnitude, respectively, of square matrices. Given a matrix, M, an iteration scheme may be employed after choosing an initial guess, v_1, for the appropriate eigenvector. For the power method successive iterates are defined by the iteration scheme,

$$v_{n+1} = M v_n, \tag{3.1}$$

while for the inverse power method successive iterates satisfy

$$M v_{n+1} = v_n. \tag{3.2}$$

Proofs that such iteration schemes give, respectively, the eigenvalue of largest and smallest magnitudes may be found in textbooks such as Jennings and McKeown [11, Chapter 9].

In the present paper we have a pair of coupled equations for θ and ψ:

$$\frac{\partial^2 \psi}{\partial x^2} + \frac{\partial^2 \psi}{\partial y^2} = \mathrm{Ra}\frac{\partial \theta}{\partial x}, \qquad \frac{\partial^2 \theta}{\partial x^2} + \frac{\partial^2 \theta}{\partial y^2} + \frac{\partial \psi}{\partial x} = 0. \tag{3.3a, b}$$

The iteration scheme which is analogous to (3.2) then takes the form

$$\frac{\partial^2\psi_{n+1}}{\partial x^2}+\frac{\partial^2\psi_{n+1}}{\partial y^2}=\frac{\partial\theta_n}{\partial x},\qquad \frac{\partial^2\theta_{n+1}}{\partial x^2}+\frac{\partial^2\theta_{n+1}}{\partial y^2}+\frac{\partial\psi_{n+1}}{\partial x}=0. \tag{3.4}$$

Iterative convergence to the desired eigensolution may be monitored by evaluating what is effectively a Rayleigh quotient,

$$\mathrm{Ra}_{n+1}=\frac{\int\int \Phi_n^2\,\mathrm{d}x\,\mathrm{d}y}{\int\int \Phi_n\Phi_{n+1}\,\mathrm{d}x\,\mathrm{d}y}, \tag{3.5}$$

where the integrations take place over the whole computational domain. The speed of convergence of the method is well-known to depend on the relative sizes of the two smallest eigenvalues. While it is possible to speed up the convergence process by 'shifting the eigenvalue', it was not found to be necessary for the cases we solved.

An initial iterate, θ_1, displaying a desired symmetry, or perhaps no symmetry at all, is chosen. Equations (3.4) were solved using a straightforward multigrid correction scheme algorithm, as described in Briggs *et al.* [12]; this ensures a particularly rapid evaluation of successive iterates. After evaluation of Ra_{n+1}, as given by (3.5), the current iterate for θ, namely θ_{n+1}, was rescaled in order to avoid successively smaller amplitudes as the iteration procedure continues. Iterative convergence was then deemed to have taken place when successive values of Ra_n first differ by less than 10^{-8}. Very accurate values of Ra were obtained by using different grids (*e.g.*, 16×16, 32×32, 64×64, $\cdots$) and employing Richardson's Extrapolation. Typically we obtain values of Ra which are correct to four decimal places.

Apart from various configurations which are easily described within a Cartesian coordinate system, we have also considered circular, semicircular, annular and elliptically shaped domains. In the first three cases we may transform Equations (3.3) into the appropriate polar coordinate form. In the third case we employed a pseudo-polar system defined by

$$x=ar\cos\phi,\qquad y=r\sin\phi. \tag{3.6}$$

Here the ellipse, which is defined by $0\le r\le\frac{1}{2}$, has diameters a in the x-direction and 1 in the y-direction. Equation (3.3a) becomes,

$$(\cos^2\phi+a^2\sin^2\phi)\frac{\partial^2\psi}{\partial r^2}+(a^2-1)\frac{\sin2\phi}{r}\frac{\partial^2\psi}{\partial r\,\partial\phi}+\frac{(\sin^2\phi+a^2\cos^2\phi)}{r^2}\frac{\partial^2\psi}{\partial\phi^2}$$

$$+\frac{(\sin^2\phi+a^2\cos^2\phi)}{r}\frac{\partial\psi}{\partial r}+(1-a^2)\frac{\sin2\phi}{r^2}\frac{\partial\psi}{\partial\phi}=\mathrm{Ra}\Big[a\cos\phi\frac{\partial\theta}{\partial r}-a^2\frac{\sin\phi}{r}\frac{\partial\theta}{\partial\phi}\Big], \tag{3.7}$$

with an equivalent form replacing Equation (3.3b).

In some of the cases we present in the next section we also rotate the x- and y-axes in order to remove certain symmetries. This will, of course, make the governing equations slightly more complicated, and we omit presentation of such modifications for the sake of brevity.

4. Numerical results and further analysis

Using the above numerical method we computed streamlines and isotherms corresponding to the onset of convection for a large number of differently shaped domains, but we restrict

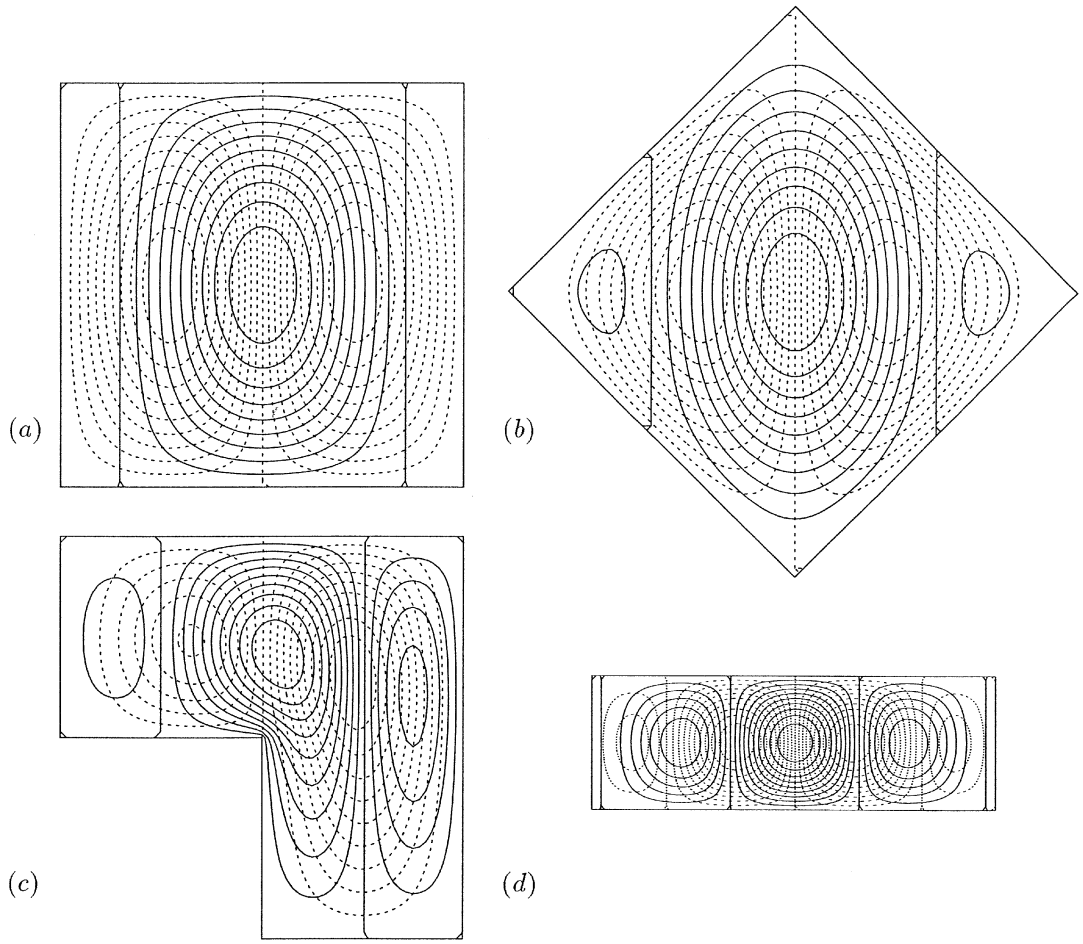

Figure 1. Streamlines and isotherms in various domains: (a) a unit square; (b) an inclined unit square; (c) an L-shaped region formed from a unit square; (d) a 3 × 1 rectangle. Continuous lines and dashed lines represent computed streamlines or the isotherms, respectively, or vice versa – this also applies to Figures 2 to 4. The critical Rayleigh number for both the square boxes is $8\pi^2$, while that for the L-shaped domain is 154·3012, and for the rectangular domain it is $\frac{40}{9}\pi^2 \backsimeq 43{\cdot}8649$.

attention to 14 cases and these are displayed in Figures 1 to 4. Contours are drawn at 20 equally spaced intervals in the range $-\Phi_e \leq \Phi \leq \Phi_e$, where $\Phi_e = \max_{ij}|\Phi_{ij}|$ is the maximum absolute value of the appropriate dependent variable, ψ or θ, over the numerical grid.

In Figure 1 we display the onset pattern for (a) a unit square, (b) a unit square rotated through 45°, (c) an L-shaped domain formed by excising a $\frac{1}{2} \times \frac{1}{2}$ square from a corner of a unit square, and (d) a 3 × 1 rectangle, which is plotted at a different scale from the other shapes. In all cases the streamlines and isotherms may be exchanged for one another, and the final solution obtained by the inverse-power method depends on the symmetry of the initial iterate. For example, for the unit square, the initial iterate for θ displays an odd symmetry, and this is maintained during the iterations. An even initial iterate yields an even converged θ field.

The critical Rayleigh numbers for cases (a) and (d) are consistent with those given by the analytical solutions for a rectangle given in [6] and [7]. Let us present the results in the

framework of the Helmholtz equation (2.20). Assume that the rectangle has length L and height H in dimensional variables. Furthermore H is the unit of dimensionless length. The aspect ratio is $a = L/H$, and we consider the domain $0 < x < a,\ 0 < y < 1$ with $F = 0$ along the entire boundary. The solution of the Helmholtz equation with the lowest eigenvalue is a simple sine both in x and y,

$$F(x, y) = \sin\frac{\pi x}{a}\sin\pi y, \tag{4.1}$$

which immediately produces the following eigenvalue and the corresponding critical Rayleigh number

$$\alpha = \sqrt{\frac{1}{a^2} + 1}, \qquad \mathrm{Ra}_c = 4\pi^2\left(\frac{1}{a^2} + 1\right). \tag{4.2a, b}$$

In terms of the present formulation we have, for case (a), where $a = 1$ implying $\alpha = \sqrt{2}$,

$$\psi = \sin\pi x\ \cos\sqrt{2}\pi x\ \sin\pi y, \qquad \theta = \left(\frac{1}{2\sqrt{2}\pi}\right)\sin\pi x\ \sin\sqrt{2}\pi x\ \sin\pi y, \tag{4.3}$$

with $\mathrm{Ra}_c = 8\pi^2$. In case (d), for which $a = 3$ and hence $\alpha = \sqrt{10/9}$,

$$\psi = \cos\frac{\pi}{3}x\ \cos\sqrt{\frac{10}{9}}\pi x\ \sin\pi y, \quad \theta = \left(\frac{1}{2\pi}\sqrt{\frac{9}{10}}\right)\cos\frac{\pi}{3}x\ \sin\sqrt{\frac{10}{9}}\pi x\ \sin\pi y, \tag{4.4}$$

with $\mathrm{Ra}_c = \frac{40}{9}\pi^2$. The respective critical values of Ra have been reproduced numerically to more than 4 decimal places and therefore we have confirmation that the numerical code works correctly for these cases.

The restriction brought about by the removal of part of the unit square in case (c) causes a substantial rise in the critical Rayleigh number. But even in this case, which displays no symmetry with respect to either the horizontal or vertical directions, there is the same degeneracy with respect to the eigensolutions.

Returning to the two unit squares, we note firstly that they correspond to precisely the same critical Rayleigh number (and, from our computations, this is also true of any other rotation of the unit square), and secondly each pair of vertical streamlines displayed in Figures 1a and 1b are of precisely the same distance apart, which was a motivation behind the substitution used in equations (2.17). We note that a solution for case (b) is

$$\psi = \cos\Big(\pi\frac{(x+y)}{\sqrt{2}}\Big)\cos\Big(\pi\frac{(y-x)}{\sqrt{2}}\Big)\cos\sqrt{2}\pi x, \tag{4.5a}$$

$$\theta = \frac{1}{2\sqrt{2}\pi}\cos\Big(\pi\frac{(x+y)}{\sqrt{2}}\Big)\cos\Big(\pi\frac{(y-x)}{\sqrt{2}}\Big)\sin\sqrt{2}\pi x. \tag{4.5b}$$

This was obtained by rotating $F(x, y)$ given in (4.1) by 45° about the origin.

Figure 2 displays two different $\frac{1}{2} \times 1$ rectangular domains and two triangles forming half of a unit square. These are placed in the same figure because all four cases have the critical Rayleigh number $20\pi^2$. Moreover, a close inspection of the vertical streamlines also suggests that they are the same distance apart in all four cases — this was noted as a general feature in the analysis above which led to the derivation of the Helmholtz equation (2.20). These features suggest that the triangular solutions must be related to the rectangular solutions.

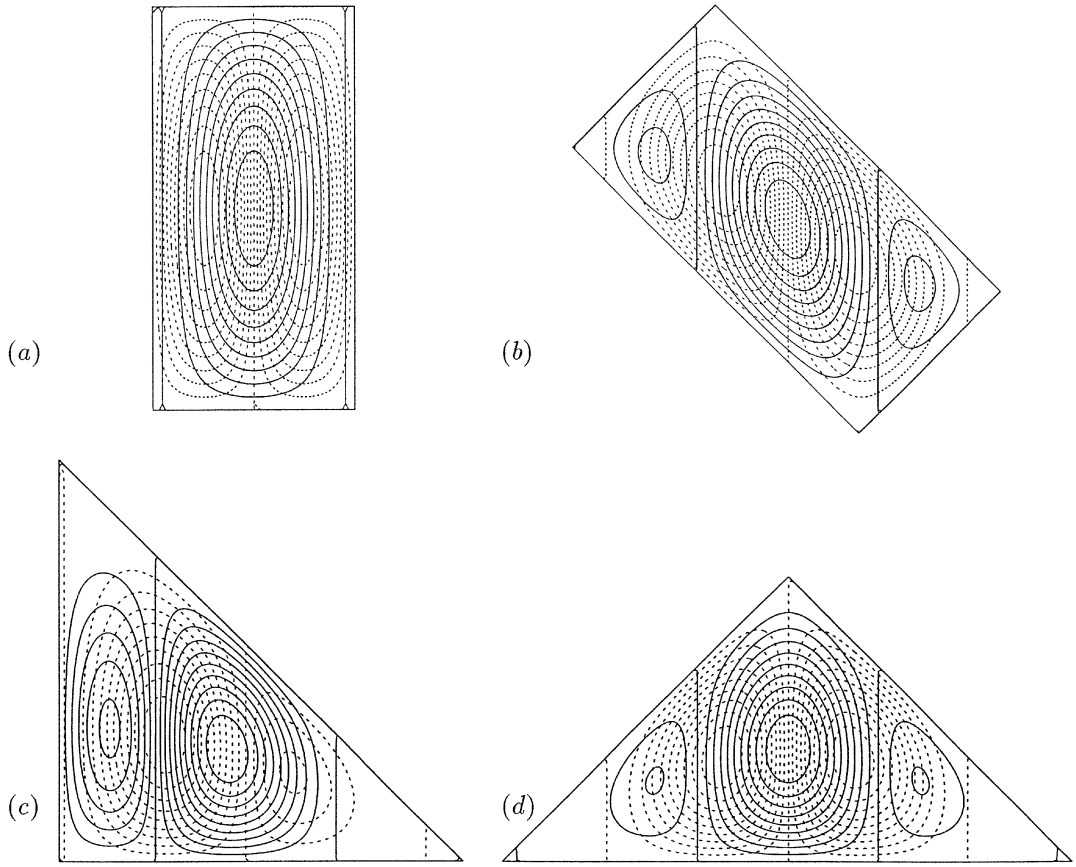

Figure 2. Streamlines and isotherms in various domains: (a) a $\frac{1}{2} \times 1$ rectangle; (b) an inclined $\frac{1}{2} \times 1$ rectangle; (c) a right-angled triangle with unit lengths sides; (d) a rotated right-angled triangle. The critical Rayleigh number in all four cases is $20\pi^2$.

The appropriate form of the solution given in (4.1) and (4.2) for a $\frac{1}{2} \times 1$ rectangle lying in the range $0 \leq x \leq \frac{1}{2}$, which is shown in Figure 2a, is,

$$\psi = \sin 2\pi x \, \cos \sqrt{5}\pi x \, \sin \pi y, \qquad \theta = \frac{1}{2\sqrt{5}\pi} \sin 2\pi x \, \sin \sqrt{5}\pi x \sin \pi y. \tag{4.6}$$

The eigenvalue α is $\sqrt{5}$, and $\mathrm{Ra}_c = 20\pi^2$. In terms of the Helmholtz equation (2.20), we have that

$$F = \sin 2\pi x \, \sin \pi y, \qquad \textit{i.e.}, \qquad \psi = \sin 2\pi x \, \cos \sqrt{5}\pi x \, \sin \pi y \tag{4.7}$$

corresponds to the vertical rectangle in Figure 2a. We may also rotate freely the coordinate directions since the Helmholtz equation (2.20) is invariant under rotation, so that an alternative solution given by

$$F = \sin 2\pi y \sin \pi x, \qquad \textit{i.e.}, \qquad \psi = \sin \pi x \cos \sqrt{5}\pi x \, \sin 2\pi y \tag{4.8}$$

corresponds to a $1 \times \frac{1}{2}$ rectangle. The rectangle which is inclined at 45° in Figure 2b now corresponds to

$$F = \sin \frac{2\pi(x+y)}{\sqrt{2}} \sin \frac{\pi(y-x)}{\sqrt{2}},$$

$$\text{i.e.} \qquad \psi = \sin\frac{2\pi(x+y)}{\sqrt{2}}\,\cos\sqrt{5}\pi x\,\sin\frac{\pi(y-x)}{\sqrt{2}}, \tag{4.9}$$

which is formed by rotating by 45° the axes of the solution for F given in (4.7).

In all three cases given by (4.7) to (4.9) the solutions for F are identical and are related solely by rotation. On the other hand, the corresponding solutions for ψ all contain the term $\cos\sqrt{5}\pi x$ which accounts for the vertical streamlines. In this way we see why the critical Rayleigh number for any chosen shape does not depend on the angle of orientation of that shape, for each solution is given by the product of a function in the x-direction and one which may be rotated freely with the domain.

As the Helmholtz equation (2.20) is linear, we may now construct the solution for the triangle given in Figure 2c by adding those solutions given in (4.7) and (4.8). After some standard manipulations it is possible to show that the appropriate solution for ψ is

$$\psi = \sin\pi x\,\sin\pi y\,\cos\frac{\pi}{2}(x+y)\,\cos\frac{\pi}{2}(x-y)\cos\sqrt{5}\pi x. \tag{4.10}$$

Once more, that part of (4.10) which multiplies $\cos\sqrt{5}\pi x$ may be rotated at will to give solutions for similar triangles at all other orientations.

Figure 3 shows our numerical solutions for a circle and a semicircle, both of unit diameter. The Helmholtz equation (2.20) may be written in polar coordinates as,

$$\frac{\partial^2 F}{\partial r^2} + \frac{1}{r}\frac{\partial F}{\partial r} + \frac{1}{r^2}\frac{\partial^2 F}{\partial \phi^2} + \alpha^2\pi^2 F = 0. \tag{4.11}$$

The solution for F which gives the smallest value of α (and hence of Ra) in a unit diameter circle is

$$F = J_0(2\lambda_0 r) \qquad \text{with} \qquad \alpha = 2\lambda_0, \tag{4.12}$$

where $\lambda_0 = 2{\cdot}404826$ is the smallest root of the zeroth order Bessel function. This yields $\mathrm{Ra} = 16\lambda_0^2 = 92{\cdot}5310$ to four decimal places, which is in perfect accord with our numerical solutions using the inverse-power method on the full linearised equations, and with the numerical series solutions of Storesletten and Tveitereid [10]. Thus the full solution for the circle is

$$\psi = J_0(2\lambda_0 r)\cos(2\lambda_0 x), \qquad \theta = J_0(2\lambda_0 r)\sin(2\lambda_0 x). \tag{4.13}$$

A similar analysis shows that the corresponding solution for the semicircle is

$$\psi = J_1(2\lambda_1 r)\,\sin\phi\,\cos 2\lambda_1 x, \qquad \theta = J_1(2\lambda_1 r)\,\sin\phi\,\sin 2\lambda_1 x, \tag{4.14}$$

where $\lambda_1 = 3{\cdot}8317$ is the first root of the first-order Bessel function, J_1. Hence $\mathrm{Ra} = 16\lambda_1^2 = 234{\cdot}912$ in this case. In the case where a circular domain has a fin extending from its centre to the circumference (at $\phi = 0$, say), then we may write ψ in terms of $J_{1/2}(2\pi r)$, or as

$$\psi = r^{-1/2}\sin(2\pi r)\sin(\phi/2)\cos(2\pi x) \tag{4.15}$$

with $\mathrm{Ra} = 16\pi^2$. We may also write down solutions for other, more general, segments of a circle using Bessel functions of fractional order; see Courant and Hilbert [13, p. 391], for example.

We may also derive the solution for annuli of unit outer diameter and an inner diameter, ϵ. The ϕ-independent solution of the Helmholtz equation (4.11) is

$$F(r) = AJ_0(\alpha\pi r) + BY_0(\alpha\pi r), \tag{4.16}$$

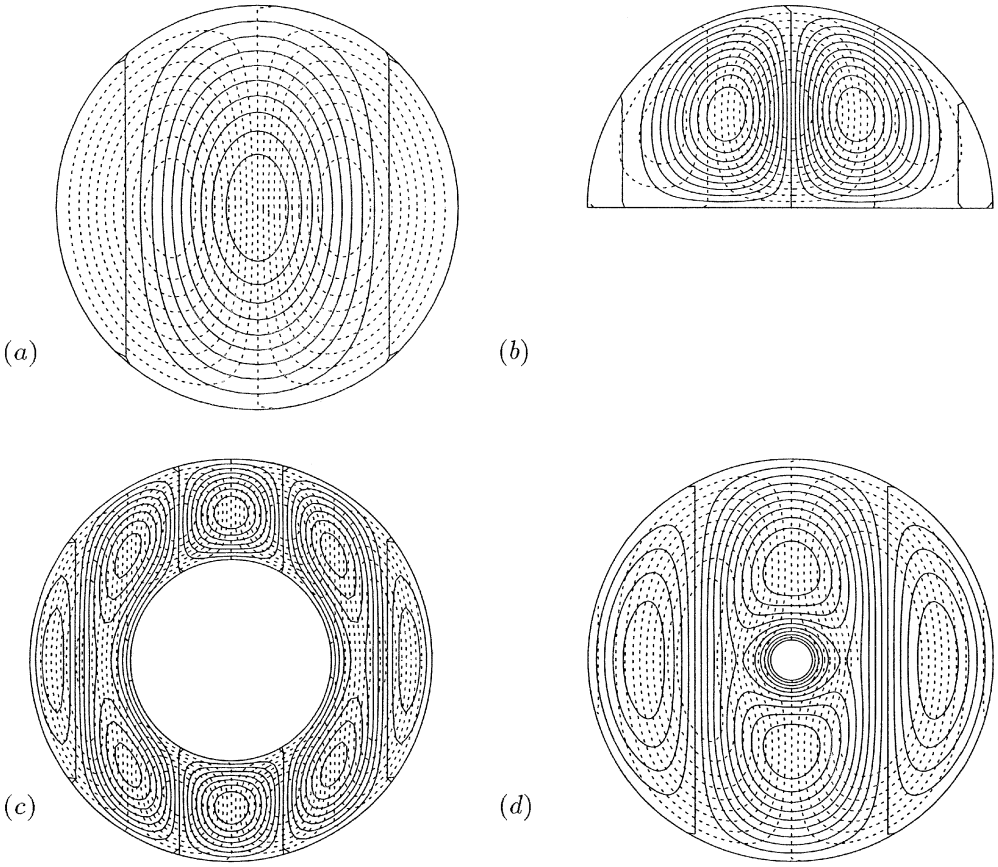

Figure 3. Streamlines and isotherms in the following domains: (a) a circle; (b) a semicircle; (c) an annulus with $\epsilon = 0{\cdot}5$; (d) an annulus with $\epsilon = 0{\cdot}1$. The respective critical Rayleigh numbers are, $16\lambda_0^2 = 92{\cdot}5310$, $16\lambda_1^2 = 234{\cdot}912$, $624{\cdot}212$ and $176{\cdot}715$.

where A and B are constants of integration and Y_0 is the zeroth-order Bessel function of the second kind. The boundary conditions are

$$F\left(\frac{1}{2}\right) = F\left(\frac{1}{2}\epsilon\right) = 0. \tag{4.17}$$

The requirement of zero determinant of the coefficient matrix gives the condition for nontrivial eigensolutions:

$$J_0(\lambda)Y_0(\epsilon\lambda) - J_0(\epsilon\lambda)Y_0(\lambda) = 0. \tag{4.18}$$

As in the circle case above we have $2\lambda = \alpha\pi$ and $\mathrm{Ra} = 16\lambda^2$. We have computed the case where the inner diameter is half the outer diameter ($\epsilon = 0{\cdot}5$) and found that $\lambda = 6{\cdot}24606$, $\alpha = 3{\cdot}97637$ and $\mathrm{Ra} = 624{\cdot}212$, which is more than six times the Rayleigh number for a full circle. This case is illustrated in Figure 3c. We see that a conducting core is strongly stabilizing, since it takes away buoyancy in the middle of the porous medium where buoyancy is most important for promoting the instability. The presence of many streamlines near the inner boundary of Figure 3d, for which $\epsilon = 0{\cdot}1$, shows how strong the effect is of having even a small hole in the circular disk. Even when $\epsilon = 1/1000$ we find a 20 per cent increase in the

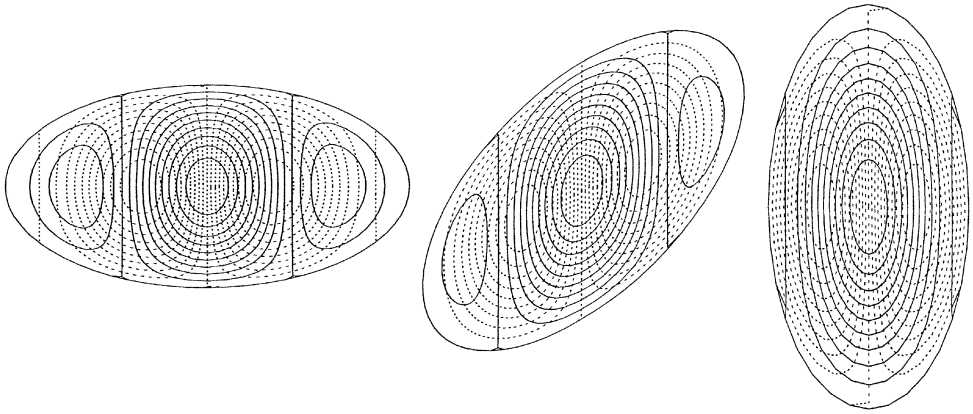

Figure 4. Streamlines and isotherms in elliptical domains of different orientations. The ellipses have major and minor axes of lengths 2 and 1. All three cases have the critical Rayleigh number 57·073.

Rayleigh number over that of the circle. The inner diameter needs to be less than 10^{-100} for the Rayleigh number to increase by less by than one per cent.

Finally we present three cases involving ellipses at various orientations in Figure 4. A full solution involves either an infinite series of sines and/or cosines in ϕ, or a product of Mathieu functions when elliptical coordinates are used (see Gladwell and Willms [14], for example), but will nevertheless retain the same cosine or sine dependence in the x-direction, as shown again by the vertical streamlines. Yet again all three have the same critical Rayleigh number.

5. Conclusions

It is known that the eigenvalue problem for the onset of convection in a two-dimensional porous cavity with zero perturbation temperature along impermeable walls is degenerate [8]. The degeneracy involves two linearly independent eigensolutions. The stream function in the first solution corresponds to the temperature perturbation in the second solution and vice versa.

The present paper explores this degeneracy further by showing that the eigenvalue problem itself degenerates into a second-order problem governed by the Helmholtz equation. The Helmholtz equation is the result of separating out a horizontal Fourier component. This separation implies that all convection cells have vertical internal cell walls. The width of each convection cells is constant, provided there are at least three cells so a cell width can be defined as the distance between two internal cell walls. The Helmholtz equation gives a critical Rayleigh number which is independent of the orientation of the porous cavity.

The wave number α of the convection cells is represented as the eigenvalue of the Helmholtz equation. The smallest possible eigenvalue for α determines the critical Rayleigh number $4\alpha^2\pi^2$. This means that the onset of convection in a porous cavity with conducting walls takes place for the greatest possible wavelength. This is different from the case of a porous rectangle with insulating sidewalls [5].

We have confirmed the degeneracy of the eigenvalue problem numerically in variously shaped domains, and compared them with exact analytical solutions. New analytical solutions have been derived for right-angled triangular, circular and semicircular cavities.

It is clear from the analysis leading to our main result that the degeneracy of the eigenvalue problem applies exclusively to flows governed by Darcy's law. The degeneracy does not apply

to Darcy-Brinkman flows or to flows in pure fluids governed by the Navier-Stokes equation. The reason for this is that the linearised equations for ψ and θ are no longer identical for these flows, and the present results rely on the fact that the stream function and perturbation temperature are multiples of one another. Preliminary work by the authors indicates that the degeneracy persists into the steady, strongly nonlinear regime, at least for rectangular cavities, but that this. However, we are quite certain that degeneracy does not exist generally in three-dimensional contexts; that this is so for the horizontal circular cylinder has already been demonstrated by Storesletten and Tveitereid [10]. Likewise, any other temperature distribution such as would be obtained by rotating the gravity vector, for example, would cause a basic flow to arise and this too destroys degeneracy. Finally, preliminary work on the use of the two-temperature model shows that the critical Rayleigh number depends on the symmetry of the disturbance for convection in rectangular cavities.

References

1. C.W. Horton and F.T. Rogers, Convection currents in a porous medium. *J. Appl. Phys.* 16 (1945) 367–370.
2. E.R. Lapwood, Convection of a fluid in a porous medium. *Proc. Camb. Phil. Soc.* 44 (1948) 508–521.
3. D.A. Nield, Onset of thermohaline convection in a porous medium. *Water Resources Res.* 11 (1968) 553–560.
4. D.A. Nield and A. Bejan, *Convection in Porous Media* (2nd edition). New York: Springer (1999) 546 pp.
5. J.L. Beck, Convection in a box of porous material saturated with fluid. *Phys. Fluids*, 15 (1972) 1377–1383.
6. T. Nilsen and L. Storesletten, An analytical study on natural-convection in isotropic and anisotropic porous channels. *Trans. A.S.M.E. J. Heat Transfer* 112 (1990) 396–401.
7. D.A.S. Rees and J.L. Lage, The effect of thermal stratification on natural convection in a vertical porous insulation layer. *Int. J. Heat Mass Transfer* 40 (1997) 111–121.
8. D.V. Lyubimov, Convective motions in a porous medium heated from below. *J. Appl. Mech. Techn. Phys.* 16 (1975) 257–261.
9. D.A. Bratsun, D.V. Lyubimov and B. Roux, Co-symmetry breakdown in problems of thermal convection in porous medium. *Physica D* 82 (1995) 398–417.
10. L. Storesletten and M. Tveitereid, Natural convection in a horizontal porous cylinder. *Int. J. Heat Mass Transfer* 34 (1991) 1959–1968.
11. A. Jennings and J.J. McKeown, *Matrix Computation* (2nd Edition). Wiley (1992) 427 pp.
12. W.L. Briggs, V.E. Henson and S.F. McCormick, *A Multigrid Tutorial* (2nd Edition). Philadelphia: S.I.A.M. (2000) 193 pp.
13. R. Courant and D. Hilbert, *Methods of Mathematical Physics* Volume 1 (2nd Edition). New York: Wiley (1953) 560 pp.
14. G.M.L. Gladwell and N.B. Willms, On the mode shapes of the Helmholtz equation. *J. Sound Vibration* 188 (1995) 419–433.